

Supporting Information

Cooperatively assembled liquid crystal enables temperature-controlled Förster resonance energy transfer

Zhen-Qiang Yu,^{*,[a]} Xiaodong Li,^[a] Wei Wan,^[b] Xin-Shun Li,^[a] Kuo Fu,^[a] Yue
Wu^{*,[a]} and Alexander D. Q. Li^{*,[b]}

^aCollege of Chemistry and Environmental Engineering, Shenzhen University, Shenzhen 518073, China

^bDepartment of Chemistry, Washington State University, Pullman, WA 99164, USA

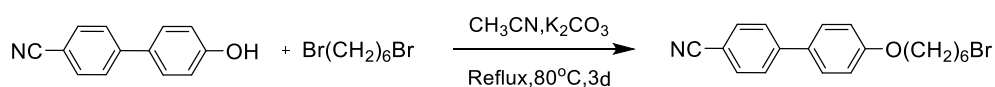
E-mail: *zqyu@szu.edu.cn; *wuyue@szu.edu.cn; *dequan@wsu.edu

Table of Contents:

1. Synthesis.....	S3
2. UV-Vis absorption and florescence intensity.....	S7
3. DSC and XRD analysis.....	S15
4. FRET between TPE-12-4CB and Nile red.....	S16
5. Characterization.....	S18

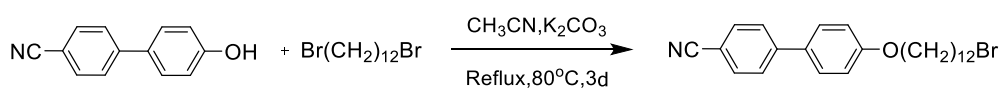
1. Synthesis

Synthesis of 4'-((6-bromohexyl)oxy)-[1,1'-biphenyl]-4-carbonitrile



4'-hydroxy-[1,1'-biphenyl]-4-carbonitrile (2.5 g, 12.8 mmol), 1,6-dibromohexane (3.6 g, 25.6 mmol) and K_2CO_3 (5.3 g, 38.4 mmol) were dissolved in 80 mL dry acetonitrile. The solution was refluxed under nitrogen. After 3 days the reaction mixture was cooled to room temperature, and acetonitrile was evaporated under reduced pressure. The mixture was dissolved in 1 M HCl (20 mL), and then extracted with CH_2Cl_2 (30 mL \times 3). The combined organic layer was washed with water and brine, dried over anhydrous Na_2SO_4 , and evaporated under reduced pressure. The crude product was purified by column chromatography (hexane/ CH_2Cl_2 = 1/1 v/v) on silica gel and obtained as a colorless powder 4'-((6-bromohexyl)oxy)-[1,1'-biphenyl]-4-carbonitrile (3.4 g, 48% yield). 1H NMR (400MHz, Chloroform-d) δ 7.73 – 7.67 (m, 2H), 7.67 – 7.61 (m, 2H), 7.53 (dd, J = 8.8, 2.1 Hz, 2H), 7.04 – 6.95 (m, 2H), 4.02 (t, J = 6.4 Hz, 2H), 3.43 (t, J = 6.8 Hz, 2H), 1.87 (ddd, J = 29.9, 8.1, 5.5 Hz, 4H), 1.53 (dq, J = 7.4, 3.4 Hz, 4H).

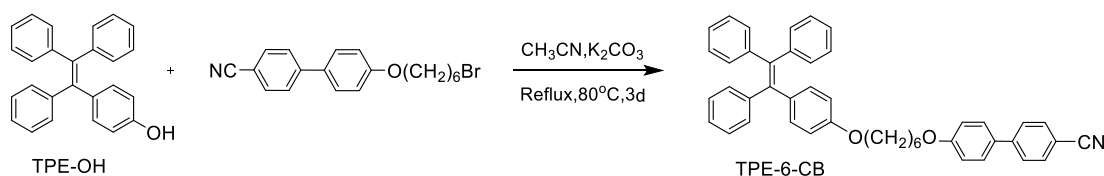
Synthesis of 4'-((12-bromododecyl)oxy)-[1,1'-biphenyl]-4-carbonitrile



4'-((12-bromododecyl)oxy)-[1,1'-biphenyl]-4-carbonitrile was synthesized

according to 4'-((6-bromohexyl)oxy)-[1,1'-biphenyl]-4-carbonitrile with 40% yield. ^1H NMR (400 MHz, Chloroform- d) δ 7.77 – 7.60 (m, 4H), 7.53 (d, J = 8.7 Hz, 2H), 6.99 (d, J = 8.8 Hz, 2H), 4.01 (t, J = 6.5 Hz, 2H), 3.41 (t, J = 6.8 Hz, 2H), 1.93 - 1.70 (m, 4H), 1.45 (dt, J = 19.4, 7.5 Hz, 4H), 1.30 (d, J = 6.7 Hz, 12H).

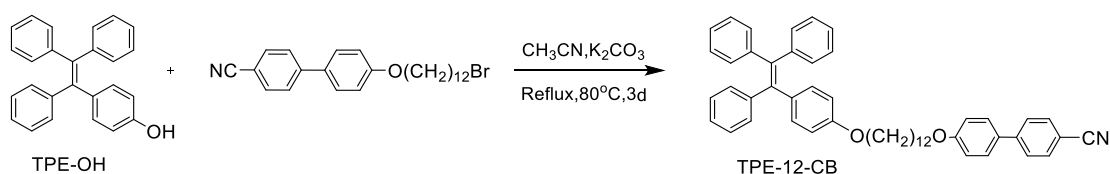
Synthesis of TPE-6-CB



1 g (2.9 mmol) TPE-OH, 1.2 g (3.5 mmol) 4'-((6-bromohexyl)oxy)-[1,1'-biphenyl]-4-carbonitrile, and 0.6 g (4.4 mmol) K_2CO_3 were dissolved in 30 mL dry acetonitrile. The solution was refluxed under N_2 . After 3 days the mixture was cooled to room temperature, H_2O was added and the mixture was extracted with CH_2Cl_2 (30 mL \times 3). The combined organic layer was washed with H_2O and brine, dried over anhydrous Na_2SO_4 , and evaporated under reduced pressure. The crude product was purified by column chromatography (hexane/ CH_2Cl_2 = 1/1 v/v) on silica gel and obtained as a colorless powder TPE-6-CB with 90% yield. ^1H NMR (400 MHz, Chloroform- d) δ 7.78 – 7.58 (m, 4H), 7.57 – 7.43 (m, 2H), 7.18 – 6.84 (m, 18H), 6.69 – 6.54 (m, 2H), 4.01 (t, J = 6.4 Hz, 2H), 3.89 (t, J = 6.4 Hz, 2H), 1.80 (dt, J = 21.9, 6.6 Hz, 4H), 1.54 (dd, J = 8.1, 4.4 Hz, 4H). ^{13}C NMR (100 MHz, Chloroform- d) δ 159.87, 157.72, 144.18, 144.10, 140.67, 140.15, 136.10, 132.68, 132.63, 131.50, 131.47, 131.45, 128.45, 127.82, 127.70, 127.20, 126.46, 126.33, 115.22, 113.69, 110.18, 68.12, 67.71, 29.37, 29.27,

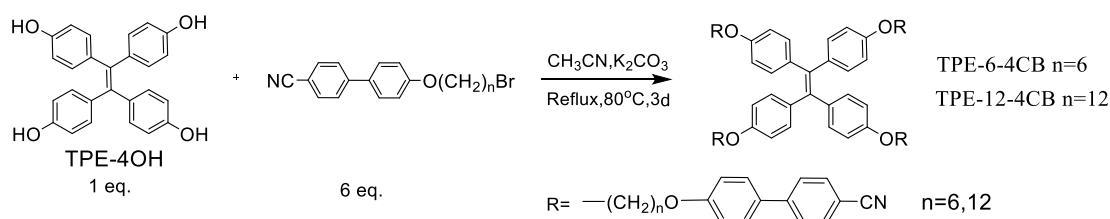
26.01. HRMS (ESI, m/z): $[M + H]^+$ calcd for $C_{45}H_{40}NO_2$ 626.3054, found 626.3053.

Synthesis of TPE-12-CB



TPE-12-CB was synthesized according to TPE-6-CB with 78.4% yield. ^1H NMR (400 MHz, Chloroform- d) δ 7.76 – 7.57 (m, 4H), 7.57 – 7.43 (m, 2H), 7.17 – 6.82 (m, 18H), 6.69 – 6.52 (m, 2H), 4.00 (t, $J = 6.5$ Hz, 2H), 3.86 (t, $J = 6.5$ Hz, 2H), 1.76 (dt, $J = 32.7, 7.4$ Hz, 4H), 1.51 – 1.17 (m, 18H). ^{13}C NMR (100 MHz, Chloroform- d) δ 157.79, 145.40, 144.18, 144.14, 140.70, 140.09, 135.99, 132.67, 132.61, 131.50, 131.47, 131.44, 128.43, 127.80, 127.69, 127.18, 126.43, 126.31, 115.21, 113.68, 110.15, 68.30, 67.92, 29.68, 29.53, 29.50, 29.43, 29.35, 26.19, 26.16. MS (ESI, m/z): $[M + H]^+$ calcd for $C_{51}H_{52}O_2N$ 710.4, found 710.7.

Synthesis of TPE-6-4CB and TPE-12-4CB



TPE-6-4CB was synthesized according to TPE-6-CB with 20% yield. ^1H NMR (400 MHz, Chloroform- d) δ 7.68 (d, $J = 8.4$ Hz, 8H), 7.63 (d, $J = 8.4$ Hz, 8H), 7.56 – 7.48 (m, 8H), 7.02 – 6.96 (m, 8H), 6.91 (d, $J = 8.2$ Hz, 8H), 6.62 (d, $J = 8.2$ Hz, 8H), 4.01 (t, $J = 6.4$ Hz, 8H), 3.90 (t, $J = 6.5$ Hz, 8H), 1.81 (dt, $J = 21.0, 6.5$ Hz, 17H), 1.54 (dd,

$J = 9.0, 4.7$ Hz, 20H). ^{13}C NMR (100 MHz, Chloroform-d) δ 159.83, 157.38, 145.31, 136.94, 132.64, 131.38, 128.42, 127.14, 115.19, 113.65, 110.13, 77.36, 77.04, 68.09, 67.69, 29.37, 29.24, 26.00, 25.98. HRMS (ESI, m/z): $[\text{M} + \text{H}]^+$ calcd for $\text{C}_{102}\text{H}_{97}\text{N}_4\text{O}_8$ 1505.7301, found 1505.7305.

TPE-12-4CB was synthesized according to TPE-6-CB with 20% yield. ^1H NMR (400 MHz, Chloroform-d) δ 7.90 – 7.56 (m, 16H), 7.51 (d, $J = 8.5$ Hz, 8H), 6.98 (d, $J = 8.4$ Hz, 8H), 6.91 (d, $J = 8.3$ Hz, 8H), 6.61 (d, $J = 8.4$ Hz, 8H), 3.99 (t, $J = 6.5$ Hz, 8H), 3.86 (t, $J = 6.6$ Hz, 8H), 1.76 (dt, $J = 30.5, 7.3$ Hz, 17H), 1.55 – 1.01 (m, 78H). ^{13}C NMR (100 MHz, Chloroform-d) δ 159.91, 145.35, 136.89, 132.63, 131.30, 128.39, 127.14, 115.19, 113.63, 77.36, 77.00, 68.27, 67.89, 29.66, 29.48, 29.33, 26.19, 26.14. HRMS (ESI, m/z): $[\text{M} + \text{H}]^+$ calcd for $\text{C}_{126}\text{H}_{145}\text{N}_4\text{O}_8$ 1842.1057, found 1842.1061.

2. UV-Vis absorption and fluorescence intensity

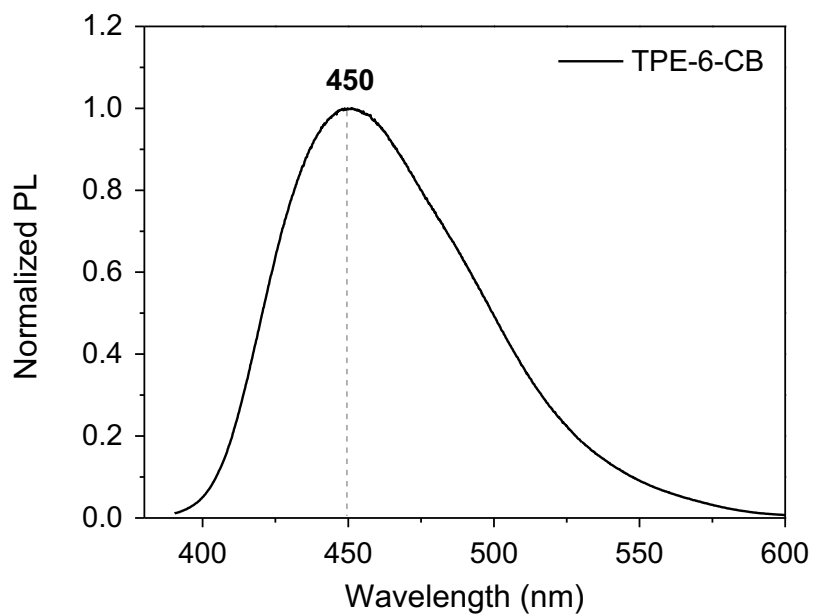


Fig. S1. Normalized fluorescence spectrum of TPE-6-CB in solid powder.

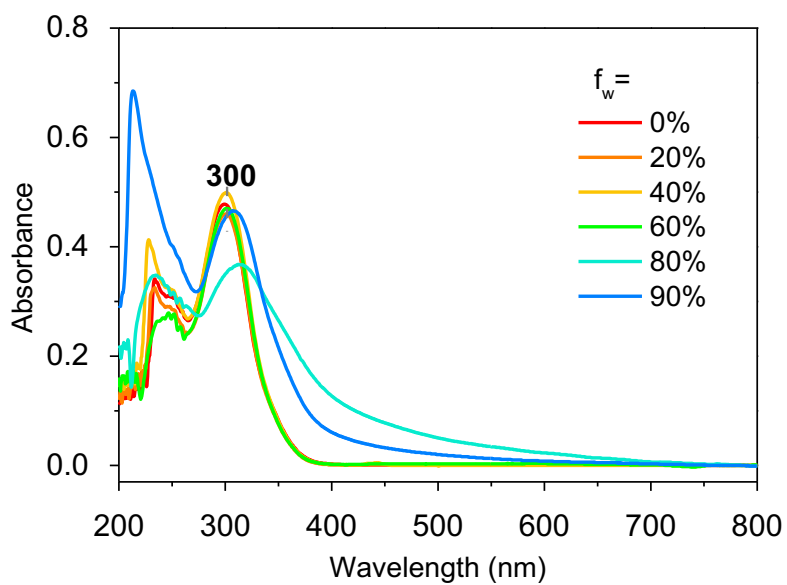


Fig. S2. Absorption spectra of TPE-6-CB in H₂O/THF mixtures with different water fractions (f_w).

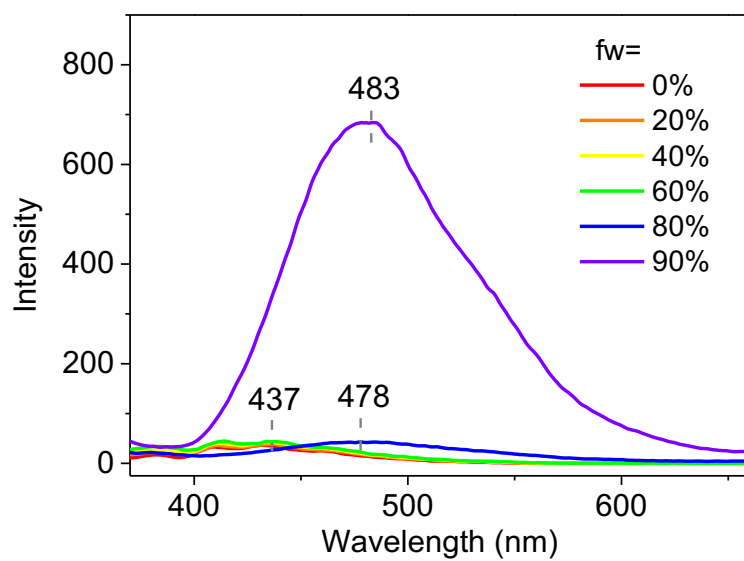


Fig. S3. Fluorescence spectra of TPE-6-CB (10 μ M) in H₂O/THF mixtures with different water fractions (f_w).

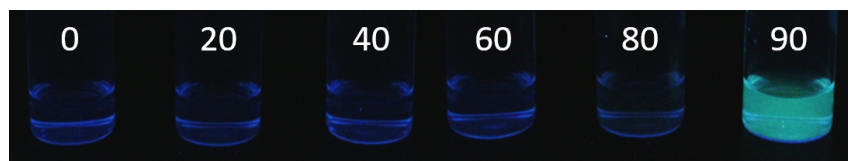


Fig. S4. Photographs of TPE-6-CB in H₂O/THF mixtures with different water fractions (f_w).

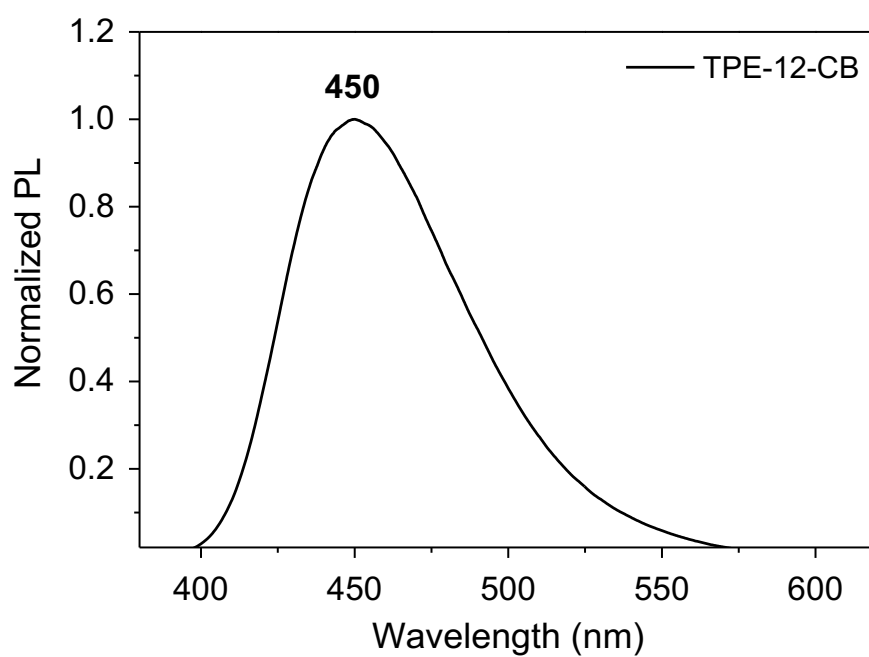


Fig. S5. Normalized fluorescence spectrum of TPE-12-CB in solid powder.

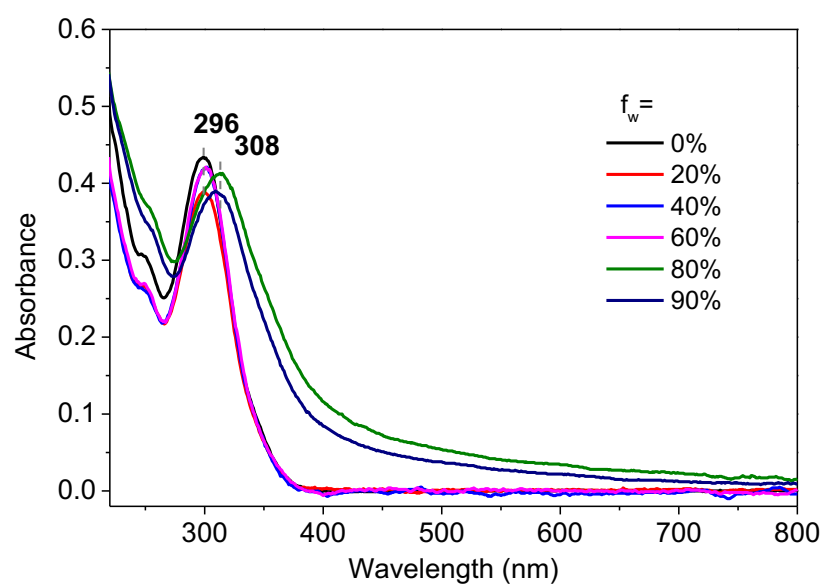


Fig. S6. Absorption spectra of TPE-12-CB in H₂O/THF mixtures with different water fractions (f_w).

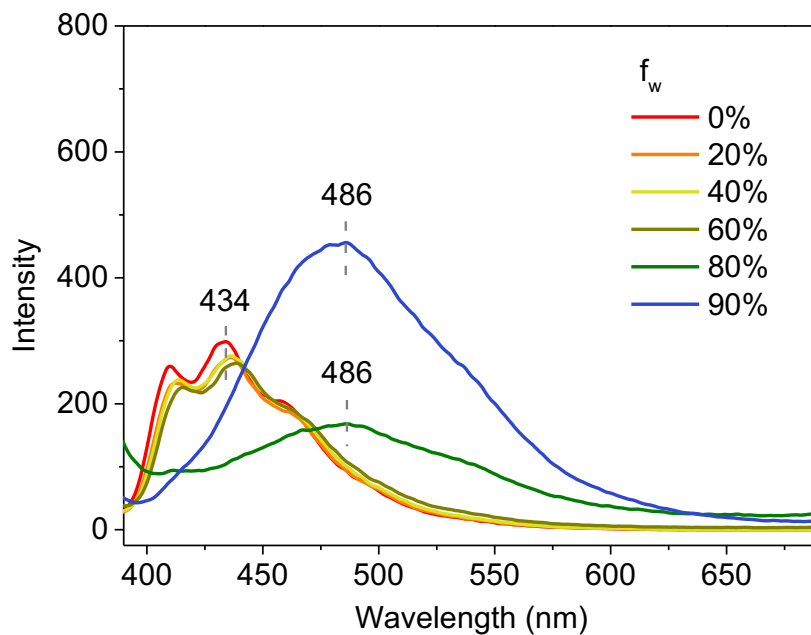


Fig. S7. Fluorescence spectra of TPE-12-CB (10 μM) in $\text{H}_2\text{O}/\text{THF}$ mixtures with different water fractions (f_w).

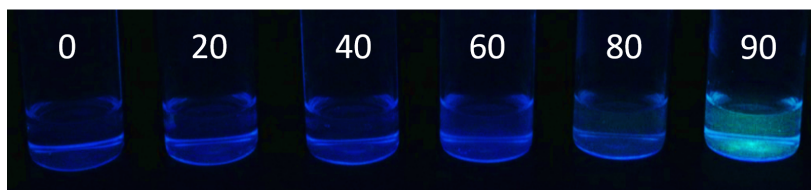


Fig. S8. Photographs of TPE-12-CB in $\text{H}_2\text{O}/\text{THF}$ mixtures with different water fractions (f_w).

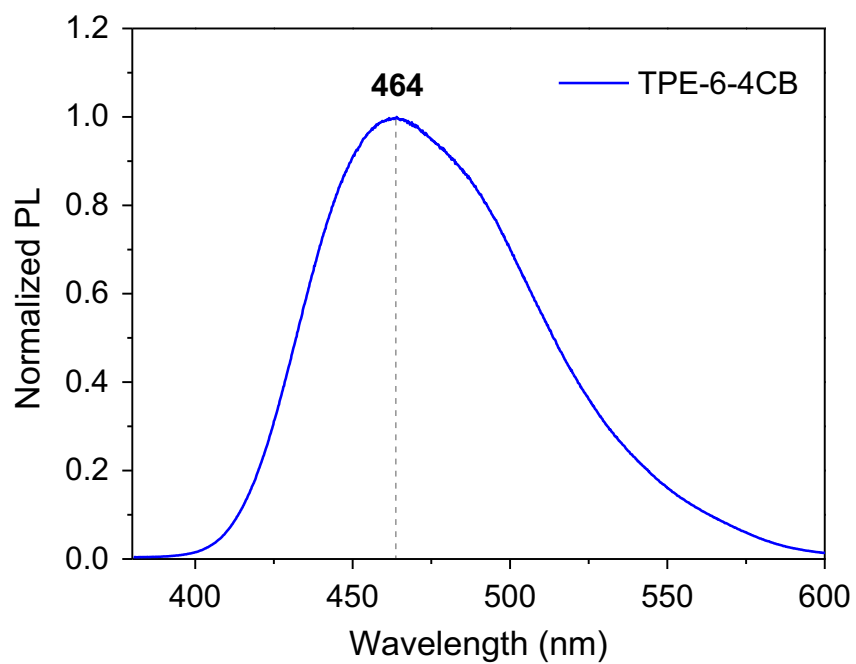


Fig. S9. Normalized fluorescence spectrum of TPE-6-4CB in solid powder.

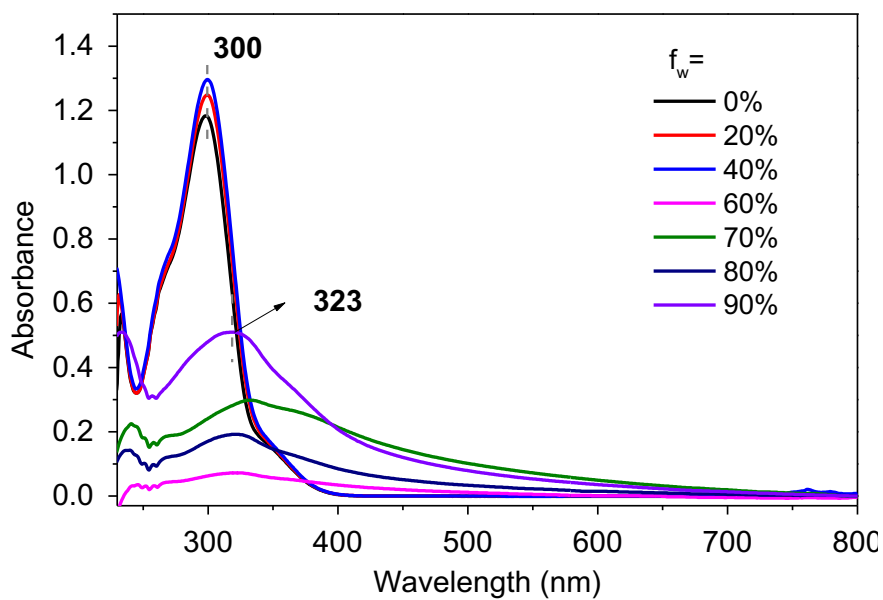


Fig. S10. Absorption spectra of TPE-6-4CB in H₂O/THF mixtures with different water fractions (f_w).

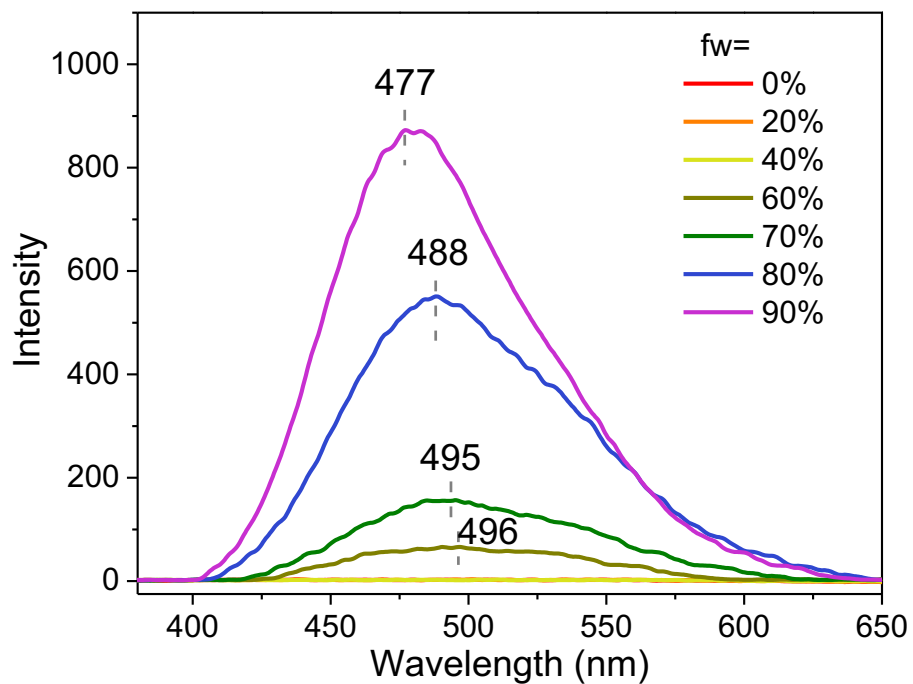


Fig. S11. Fluorescence spectra of TPE-6-4CB (10 μ M) in H₂O/THF mixtures with different water fractions (f_w).

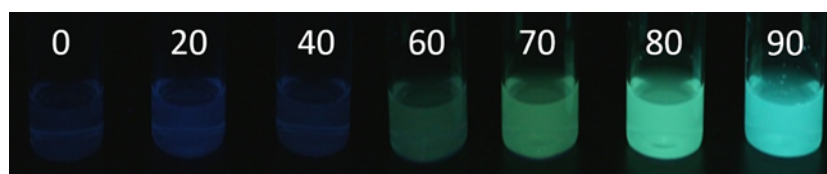


Fig. S12. Photographs of TPE-6-4CB in H₂O/THF mixtures with different water fractions (f_w).

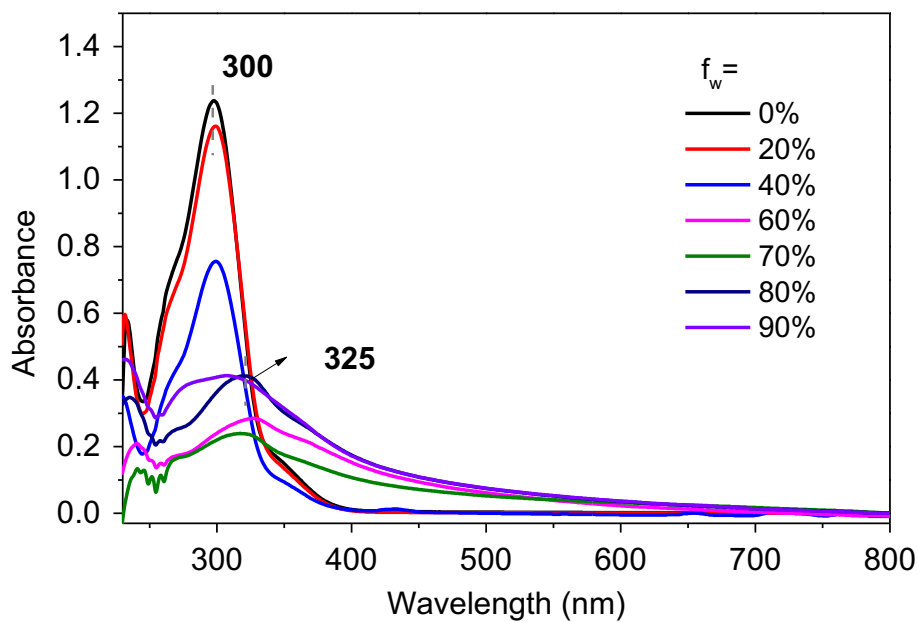


Fig. S13. Absorption spectra of TPE-12-4CB in H₂O/THF mixtures with different water fractions (f_w).

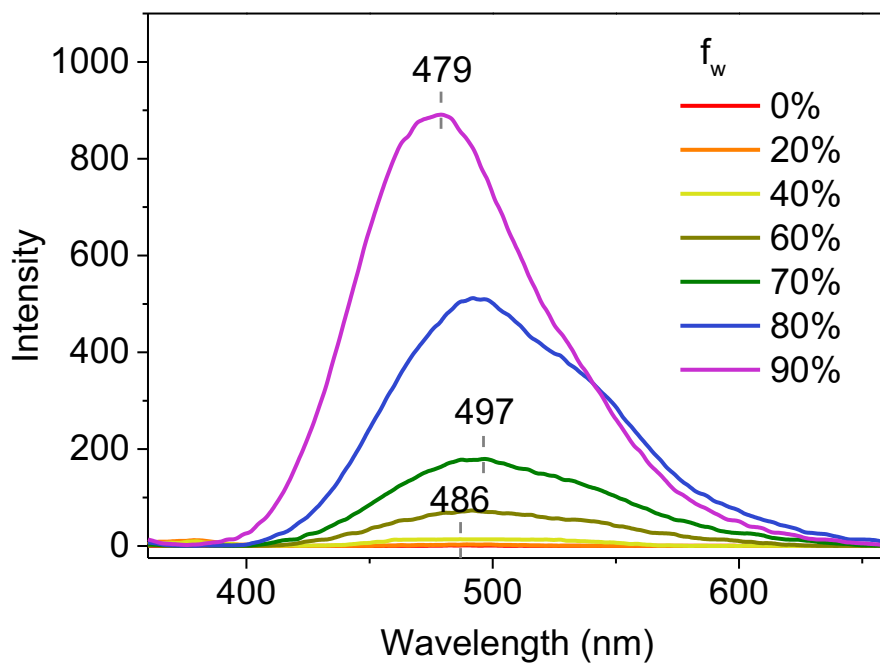


Fig. S14. Fluorescence spectra of TPE-12-4CB (10 μM) in H₂O/THF mixtures with different water fractions (f_w).

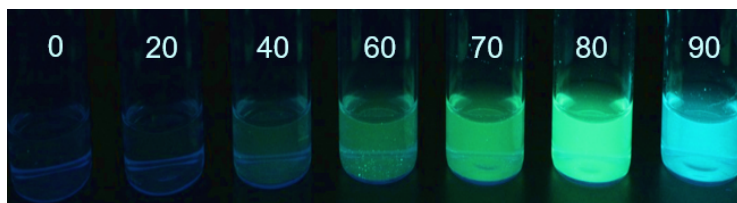


Fig. S15. Photographs of TPE-12-4CB in H₂O/THF mixtures with different water fractions (f_w).

3. DSC and XRD of TPE-12-4CB analysis

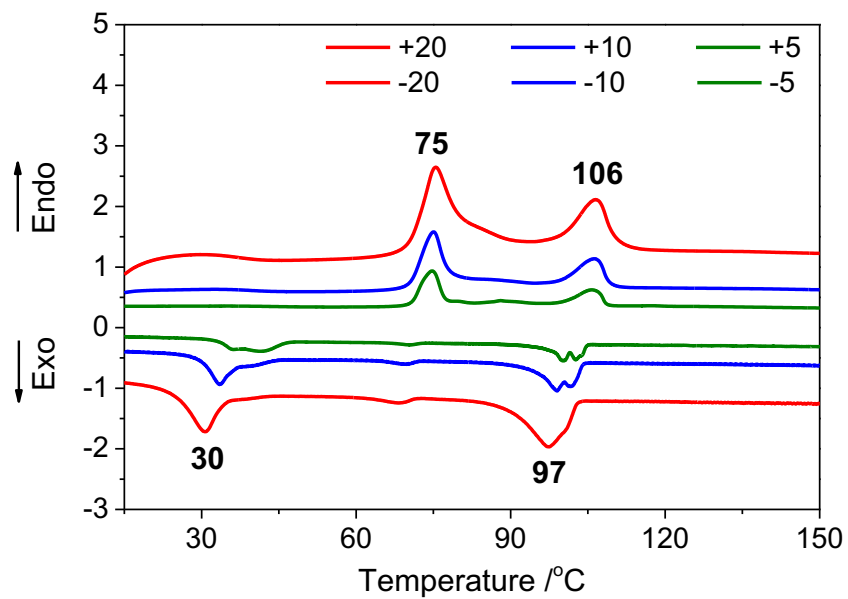


Fig. S16. DSC curves of TPE-12-4CB at heating and cooling processes in N₂ atmosphere.

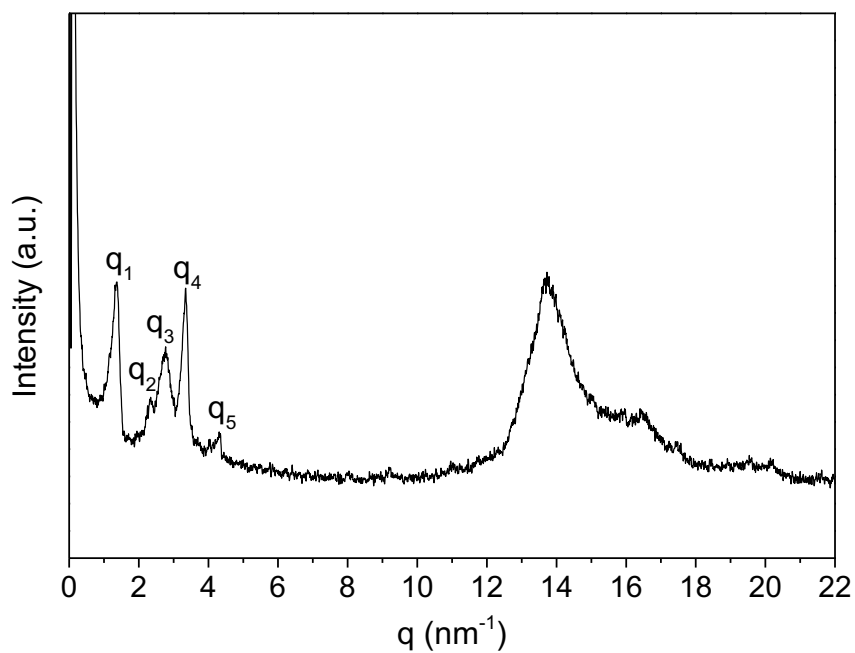


Fig. S17. XRD of TPE-12-4CB.

4. FRET between TPE-12-4CB and Nile red

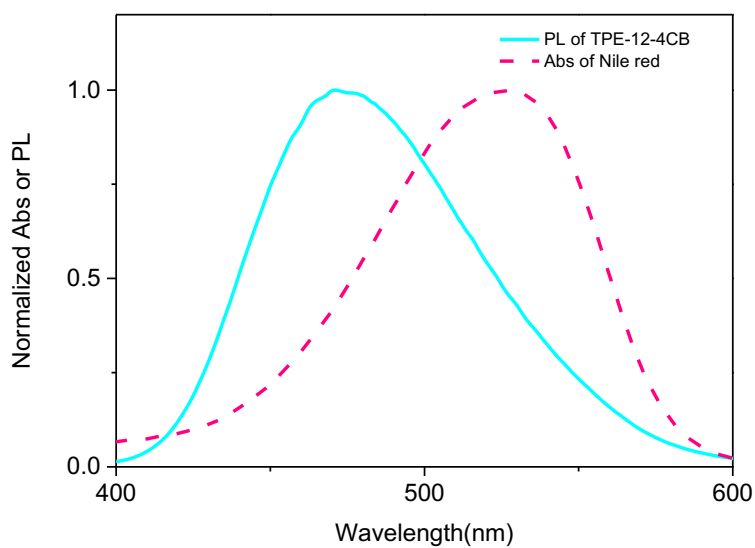


Fig. S18. Normalized absorption spectrum of Nile red and fluorescence spectrum of TPE-12-4CB

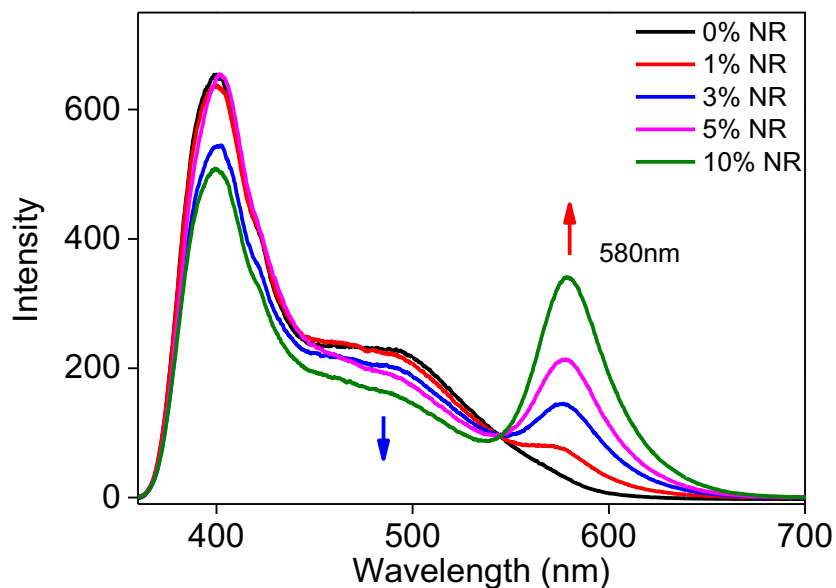


Fig. S19. FRET intensity changes of TPE-12-4CB (10^{-3} M) mixed with various Nile red molar ratio in THF ($\lambda_{\text{ex}} = 330$ nm, 25°C).

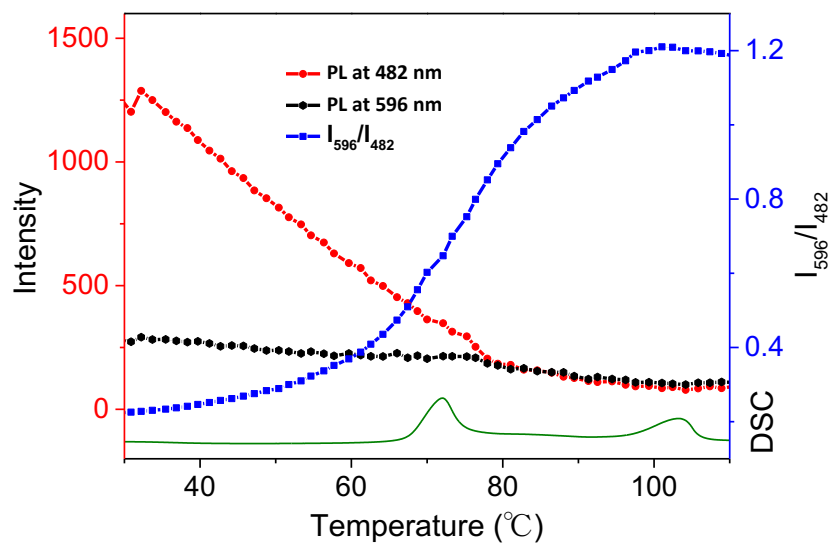


Fig. S20. Temperature-responsive fluorescence intensity at 482 and 596 nm, intensity ratio (I_{596}/I_{482}), and DSC trace of TPE-12-4CB. Note: Nile red/TPE-12-4CB = 0.1% w/w.

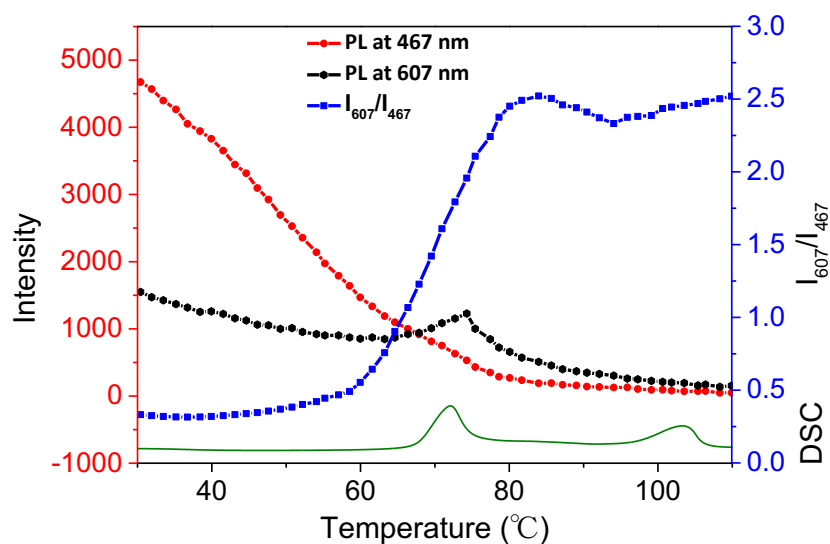
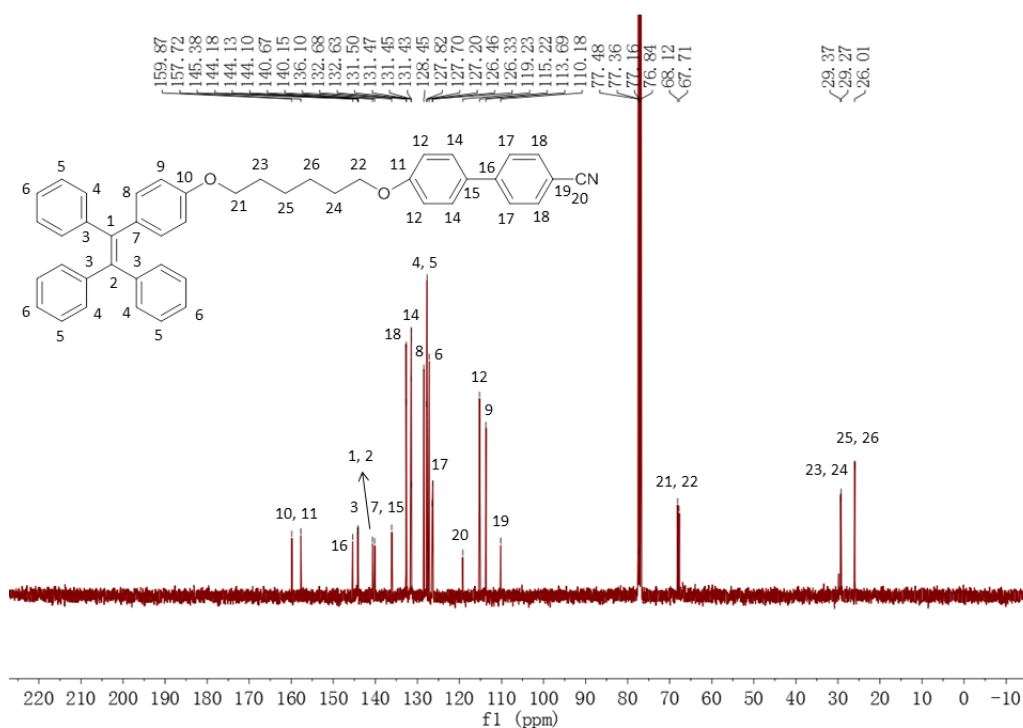
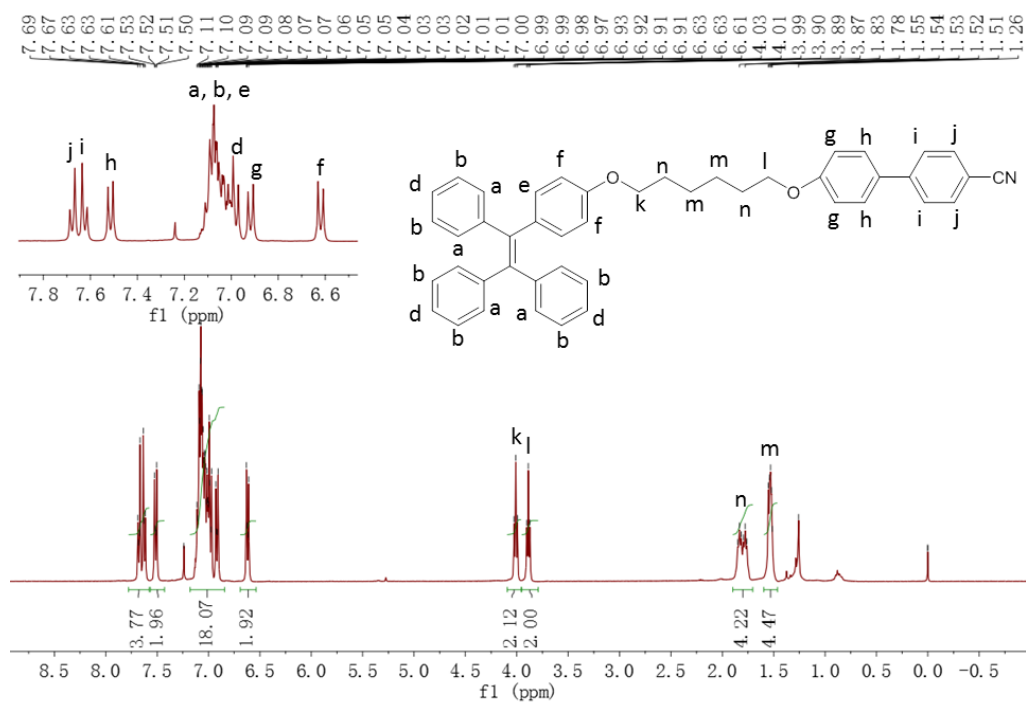


Fig. S21. Temperature-responsive fluorescence intensity at 482 and 596 nm, intensity ratio (I_{596}/I_{482}), and DSC trace of TPE-12-4CB. Note: Nile red/TPE-12-4CB = 0.5% w/w.

5. Characterization



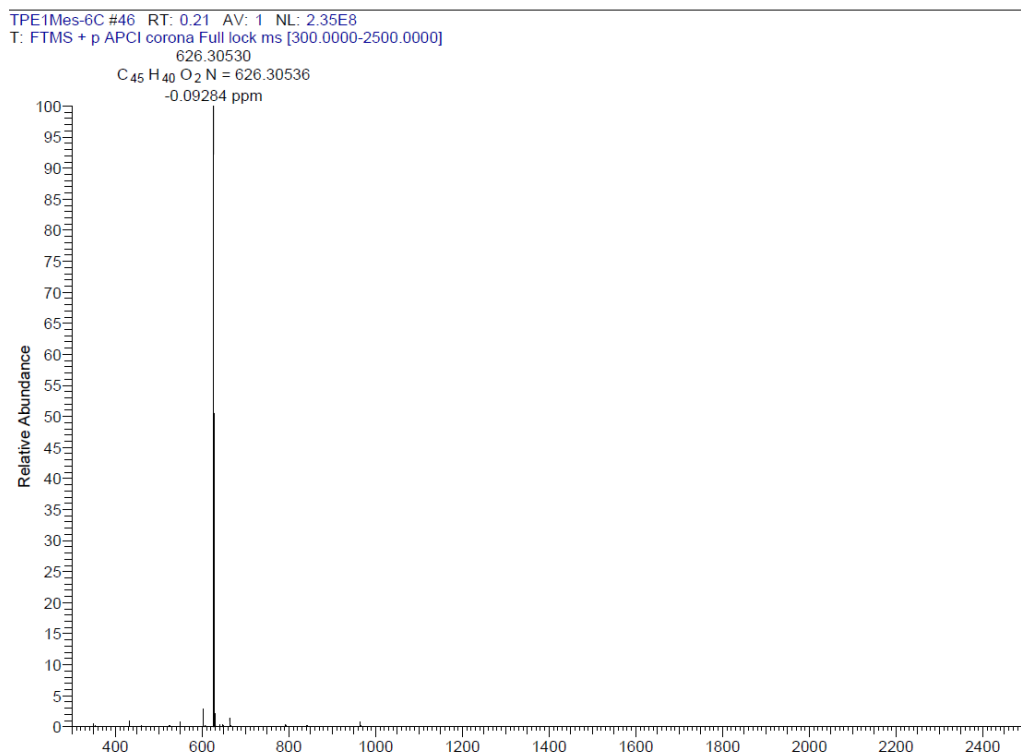


Fig. S24. HRMS of TPE-6-CB.

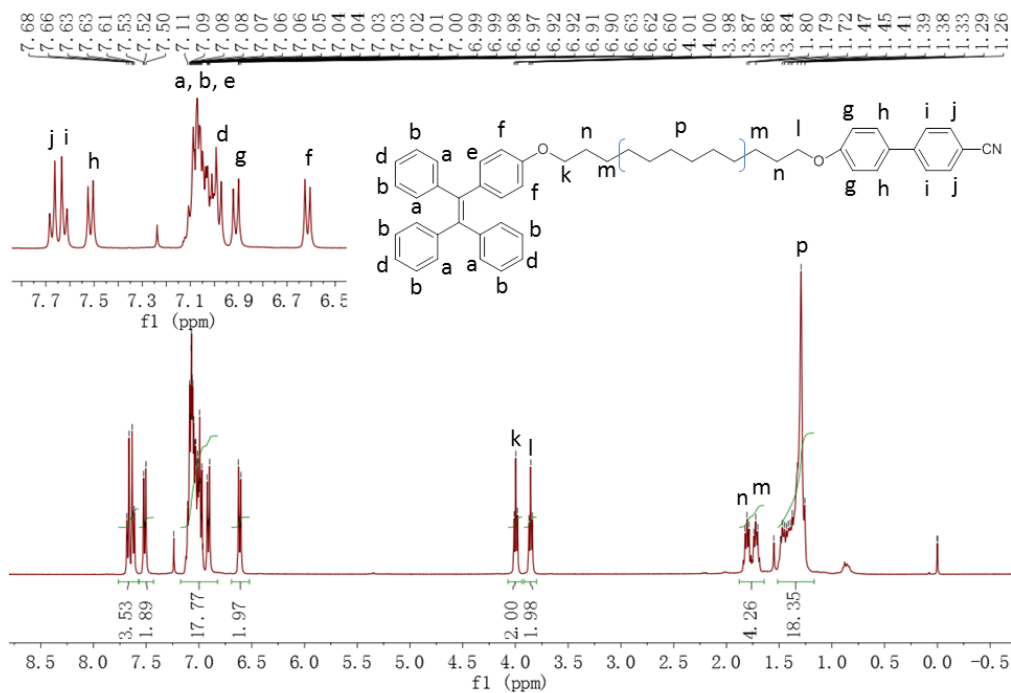


Fig. S25. ¹H NMR of TPE-12-CB in CDCl₃.

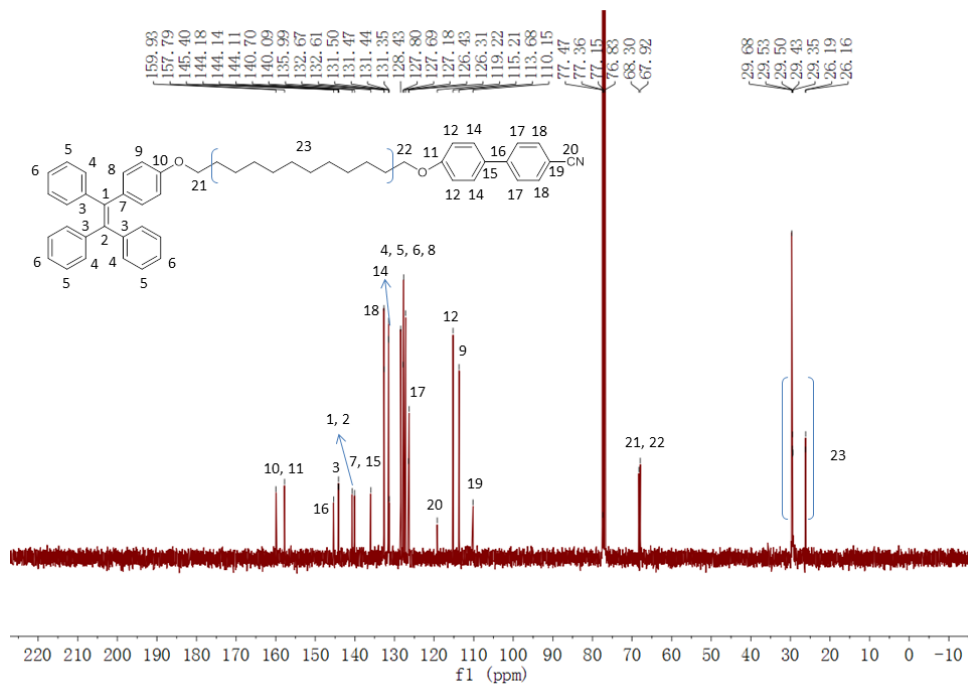


Fig. S26. ^{13}C NMR of TPE-12-CB in CDCl_3 .

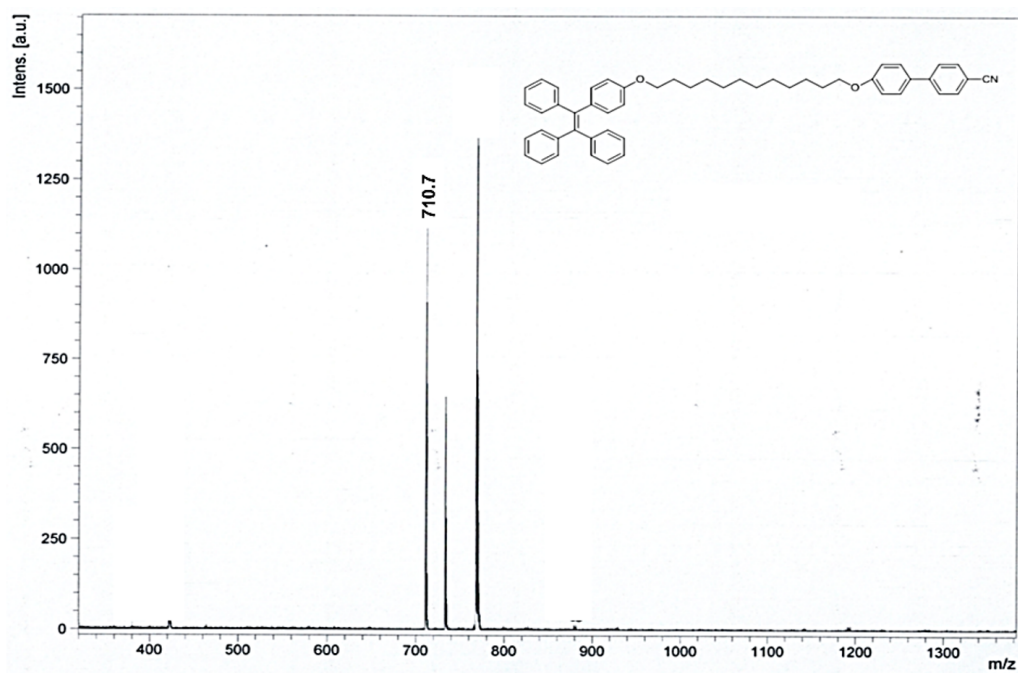


Fig. S27. MS of TPE-12-CB.

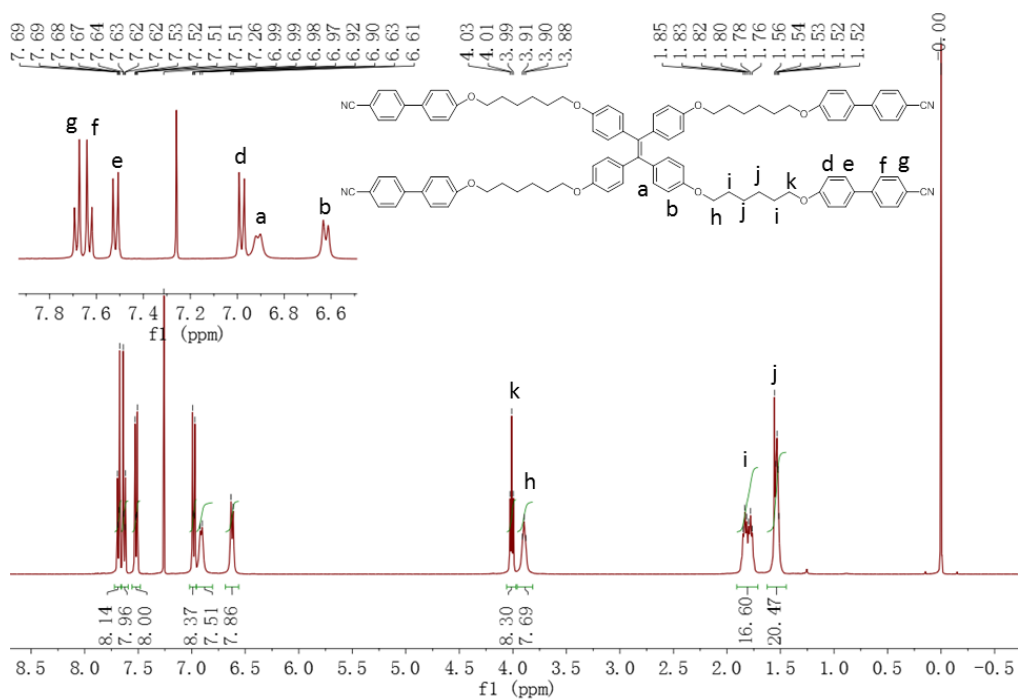


Fig. S28. ^1H NMR of TPE-6-4CB in CDCl_3 .

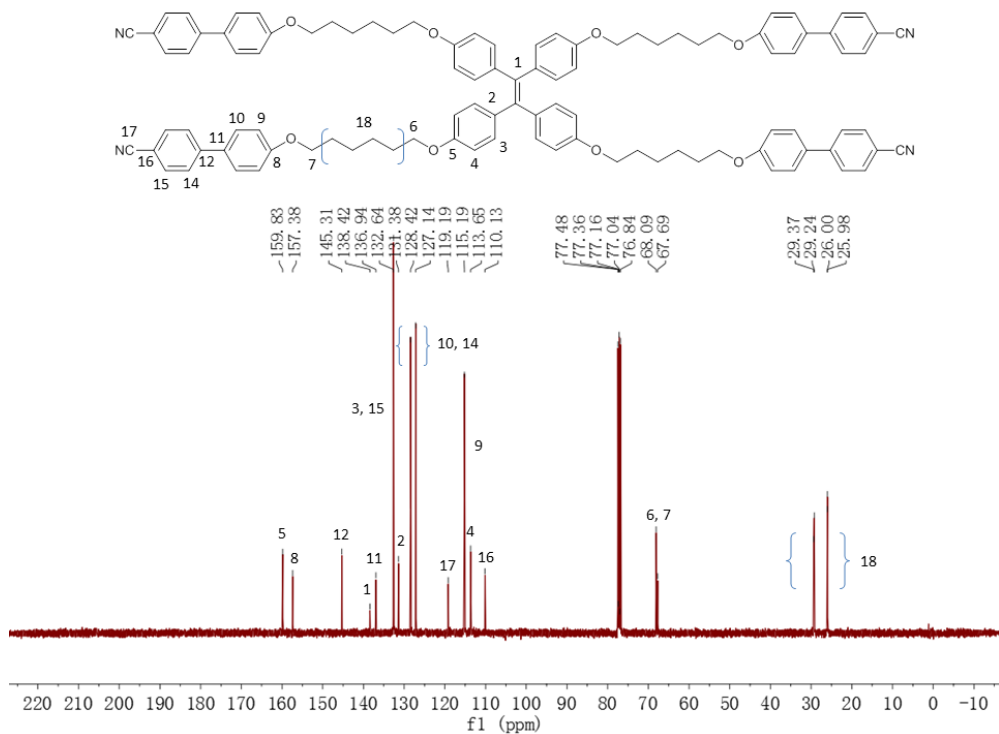


Fig. S29. ^{13}C NMR of TPE-6-4CB in CDCl_3 .

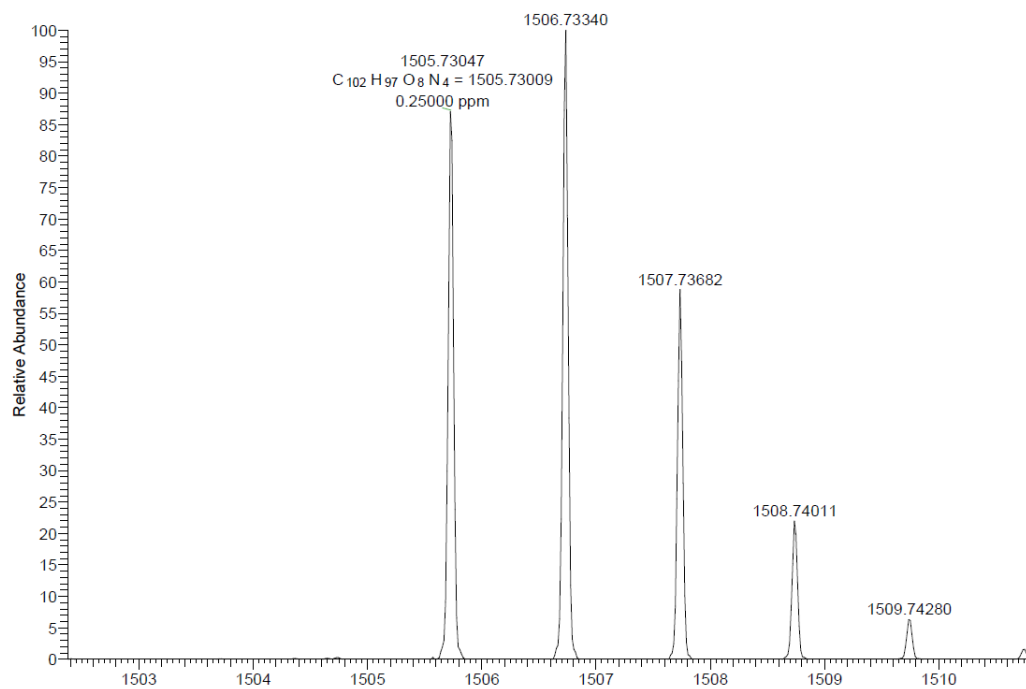


Fig. S30. HRMS of TPE-6-4CB.

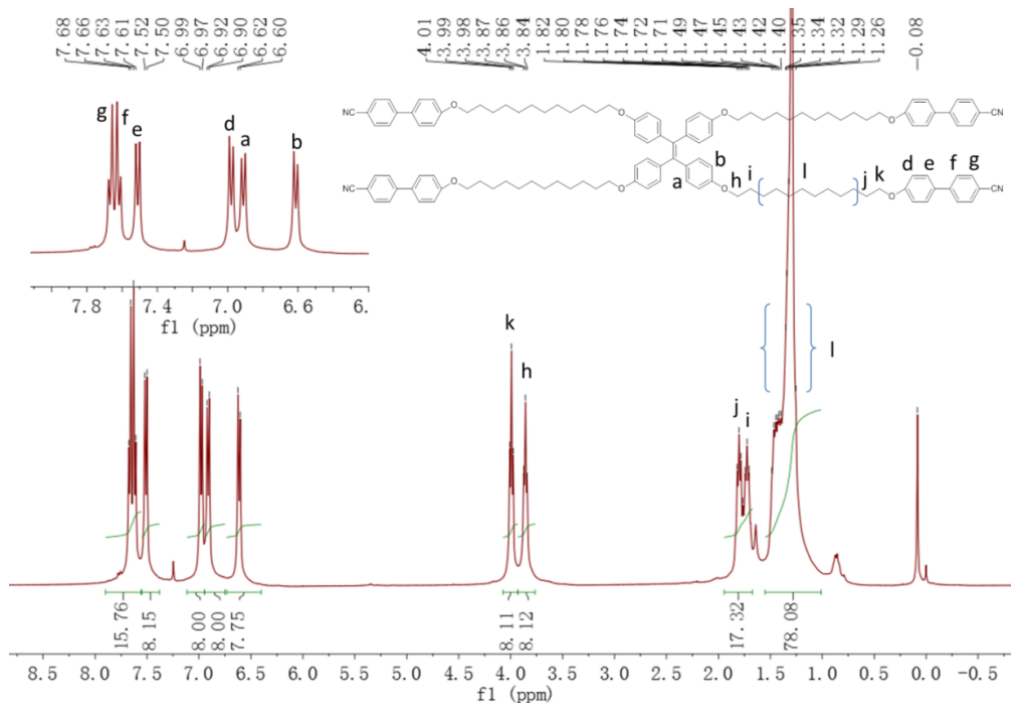


Fig. S31. ¹H NMR of TPE-12-4CB in CDCl₃.

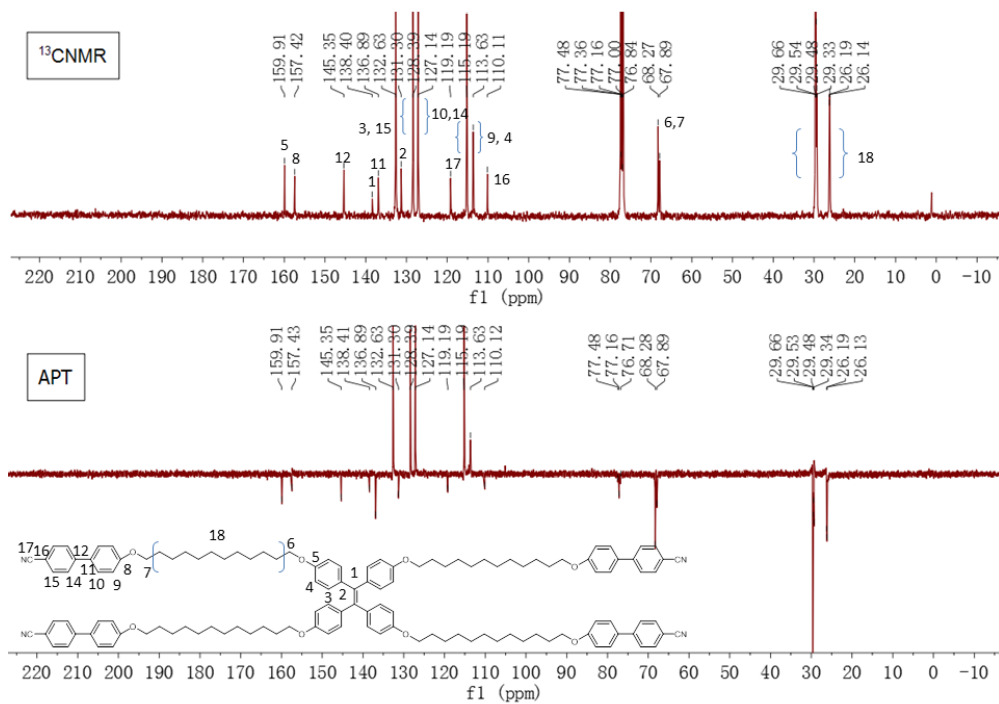


Fig. S32. ¹³C NMR of TPE-12-4CB in CDCl₃.

TPE4Mes-12C #16 RT: 0.07 AV: 1 NL: 1.49E7
 T: FTMS + p APCI corona Full lock ms [300.0000-2500.0000]

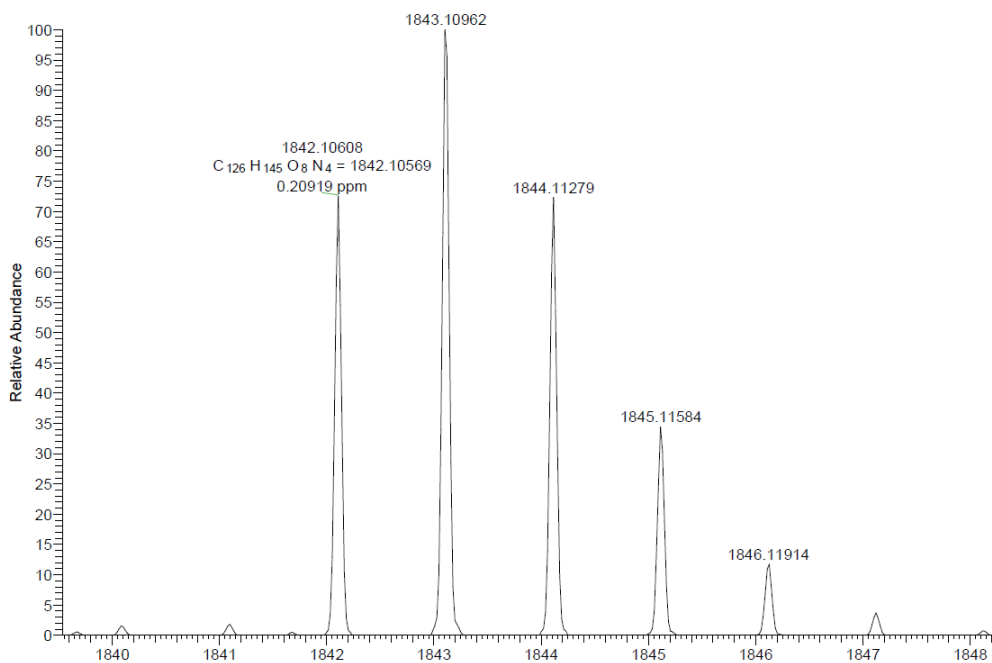


Fig. S33. HRMS of TPE-12-4CB.